Anticancer Activity of Isoobtusilactone A from *Cinnamomum kotoense*: Involvement of Apoptosis, Cell-Cycle Dysregulation, Mitochondria Regulation, and Reactive Oxygen Species

Chung-Yi Chen,[†] Ching-Hsein Chen,[§] Yi-Ching Lo,[‡] Bin-Nan Wu,[‡] Hui-Min Wang,[⊥] Wen-Li Lo,[†] Chuan-Min Yen,*[,△] and Rong-Jyh Lin*[,△]

School of Medicine and Health Sciences, Fooyin University, Kaohsiung County 831, Taiwan, Graduate Institute of Biomedical and Biopharmaceutical Sciences, College of Life Sciences, National Chiayi University, 300 University Road, Chiayi 600, Taiwan, Department and Graduate Institute of Pharmacology, College of Medicine, Kaohsiung Medical University, Kaohsiung 807, Taiwan, Faculty of Fragrance and Cosmetics, Kaohsiung Medical University, Kaohsiung 807, Taiwan, and Department of Parasitology and Institute of Medicine, College of Medicine, Kaohsiung Medical University, Kaohsiung 807, Taiwan, Republic of China

Received November 2, 2007

In this study, we investigate the anticancer effect of isoobtusilactone A (IOA), a constituent isolated from the leaves of *Cinnamomum kotoense*, on human non-small cell lung cancer (NSCLC) A549 cells. IOA was found to induce the arrest of G2-M phase, induce apoptosis, increase sub-G1, and inhibit the growth of these cells. Further investigation revealed that IOA's blockade of the cell cycle was associated with increased levels of p21/WAF1, $p27^{kip1}$, and p53. In addition, IOA triggered the mitochondrial apoptotic pathway, as indicated by an increase in Bax/Bcl-2 ratios, resulting in a loss of mitochondrial membrane potential, release of cytochrome *c*, activation of caspase-9 and caspase-3, and cleavage of PARP. We also found the generation of reactive oxygen species (ROS) to be a critical mediator in IOA-induced inhibition of A549 cell growth. In antioxidant and NO inhibitor studies, we found that by pretreating A549 cells with either *N*-acetylcystenine (NAC), catalase, mannitol, dexamethasone, trolox, or L-NAME we could significantly decrease IOA production of ROS. Moreover, using NAC to block ROS, we could significantly suppress IOA-induced antiproliferation, antimigration, and anti-invasion. Finally, we found that IOA inhibited the migration and invasion of A549 cell migration and invasion. Taken together, these results suggest that IOA has anticancer effects on A549 cells.

Cinnamomum kotoense Kanehira & Sasaki (Lauraceae) is a small evergreen tree native to Lanyu Island, a small island off the southeast coast of Taiwan. Only a few papers describe the constituents, pharmacological effects, and antiproliferation and antitumor activity of this species.[1–4] Previous studies have shown that isoobtusilactone A (IOA) (Figure 1) exhibits cytotoxic activity against MCF-7 and MDA-MB-231 (two human breast cancers), Hep G2 (a human hepatoma), and P-388 (a mouse lymphoid leukemia) as well as genotoxic effects on CHO-K1 (Chinese hamster ovary) and HTC (rat hepatoma).[2,3,5,6] IOA is a butanolide constituent isolated from the leaves of *C. kotoense*. Although some butanolide compounds have been demonstrated to have significant cytotoxicity against cancer cell lines *in vitro,* little is known about the mechanisms underlying their antitumor effects on lung cancer.

Lung cancer is one of the most common malignant and devastating of human tumors. In Taiwan, it is the first and second most common cause of mortality in women and men, respectively. Non-small cell lung cancer (NSCLC) A549 cells commonly develop resistance to radiation and chemotherapy,[7,8] and they often present at stages beyond surgical remedy. Since the current treatment modalities are inadequate, new therapies are needed to help reduce the effects of the increasing incidence in pulmonary neoplasm.[8] Chemotherapy is one of the curative strategies currently used to treat cancer, particularly metastasis. Nevertheless, a great number of tumor histotypes show a low or very low response to such treatment, and only some tumor histotypes display optimal results after its application. This is the main reason that the search for new anticancer compounds, more effective in unresponsive tumors, with reduced adverse effects and with new and original mechanisms of action, is considered an important and crucial step in improving the general outcome of cancer chemotherapy.[9,10] Many compounds that are used in cancer chemotherapy, e.g., *Vinca* alkaloids, camptothecin, and etoposide, are derived from plant sources. Therefore, we started the screening of both known and new compounds derived from plant sources that might be applied to cancer treatment.

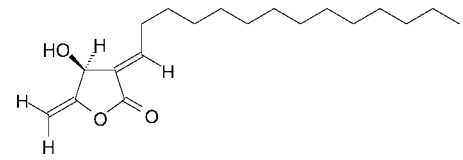

Figure 1. Chemical structure of isoobtusilactone A (IOA).

To better understand the mechanisms underlying IOA's anticancer activity, we performed assays to observe cell proliferation, cell-cycle distribution, and levels of cell cycle control-related (p53, p21/WAF1, and $p27^{kip1}$) and apoptosis-associated (Bax, Bcl-2, cytochrome *c*, caspase-9, caspase-3, and nucleosome) molecules. These factors have been strongly associated with the programmed cell death signal transduction pathway and are known to affect the chemosensitivity. This study is the first to determine the cell growth inhibition activity of IOA and to examine its effect on cell-cycle distribution, apoptosis, ROS production, and both antimigration and anti-invasion properties in human NSCLC A549 cells.

Results and Discussion

Effects of IOA on Antiproliferation and Cytotoxicity in A549 Cells. IOA was purified from leaves of *C. kotoense*, and the identity of the isolated material was confirmed by spectroscopic methods according the Experimental Section description. In the first series of experiments, an MTT test was used to study IOA ability to alter antiproliferation of lung cancer cell line A549. As shown in Figure 2A, the proliferative inhibitory effects of IOA were

* To whom correspondence should be addressed. Tel: +886-7-3121101, ext. 2334. Fax: +886-7-3218309. E-mail: rjlin@kmu.edu.tw.
[†] School of Medicine and Health Sciences, Fooyin University.
[§] Graduate Institute of Biomedical and Biopharmaceutical Sciences, National Chiayi University.
[‡] Department and Graduate Institute of Pharmacology, Kaohsiung Medical University.
[⊥] Faculty of Fragrance and Cosmetics, Kaohsiung Medical University.
[△] Department of Parasitology and Institute of Medicine, College of Medicine, Kaohsiung Medical University.

10.1021/np070620e CCC: $40.75
Published on Web 05/20/2008

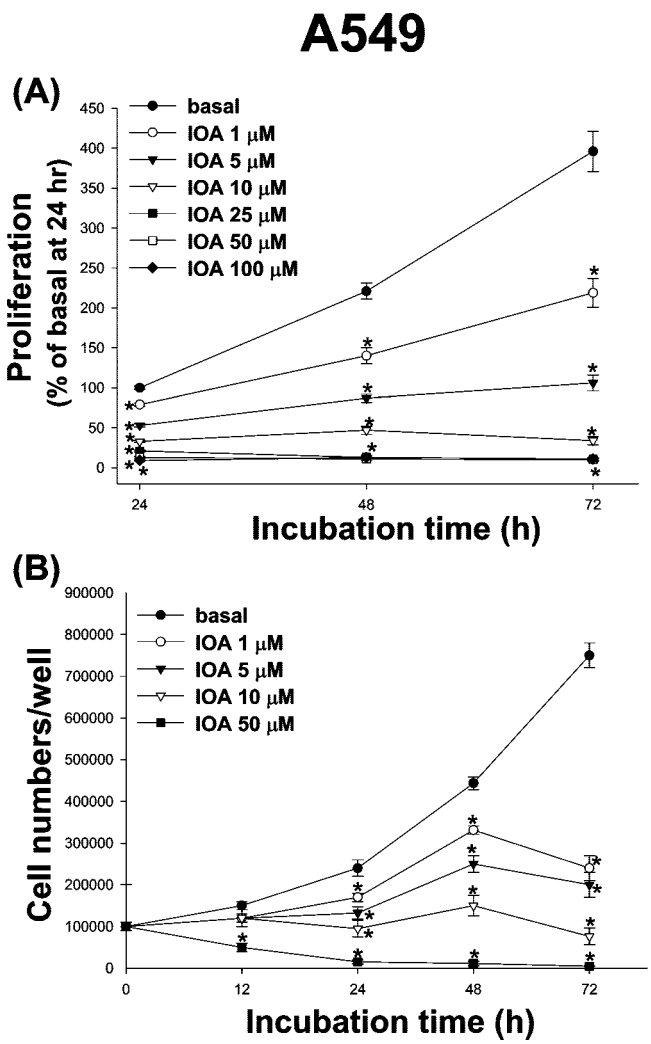

Figure 2. Antiproliferative and cytotoxic effect of IOA on A549 cells. (A) Cell proliferation was determined by MTT assay after incubation with various concentrations of IOA at 24, 48, and 72 h, respectively. Results are expressed as the percent of the cell proliferation of control at 24 h. (B) Cell viability under different concentrations of IOA at 12, 24, 48, and 72 h, respectively. Cell numbers were calculated using hemocytometers. Each value represents the mean ± SE. Statistically significant, $*p < 0.05$ to control group. ANOVA followed by Dunnett's test.

observed to be dose- and time-dependent. The maximum proliferative inhibition of IOA was 2.75 ± 0.08%, which occurred at 72 h using 100 μM IOA. Similar results were also obtained when we evaluated the cytotoxic effect of IOA by the TB dye exclusion assay (Figure 2B). In A549 cells, the IC_{50} (μM) ($-\log IC_{50} = 5.38 \pm 0.03$, 6.05 ± 0.04, and 6.14 ± 0.08 for 24, 48, and 72 h, respectively) values were, on average, lower than those observed by the MTT assay ($-\log IC_{50} = 5.29 \pm 0.03$, 5.71 ± 0.08, and 5.99 ± 0.02 for 24, 48, and 72 h, respectively).

Effects of IOA-Induced Cell-Cycle Arrest and Apoptosis. IOA at 50 μM was found to significantly increase the hypodiploid population of the cells from 1.73% to 16.69%, 36.73%, and 54.08% compared with vehicle (contains 1% DMSO in sterilized distilled H_2O) after 24, 48, and 72 h treatment, respectively (Figure 3A). This effect was enhanced when A549 cells were treated with 100 μM IOA (25.63%, 47.64%, and 60.25% cell population in sub-G1 at 24, 48, and 72 h, respectively). IOA (50 μM) was also found able to increase the S-G2/M phase. In addition, IOA (100 μM) decreased the accumulation of cells in S phase from 35.82% (vehicle) to 16.24% with a concomitant increase of the G2/M phase at 72 h.

Apoptosis Assays of Morphological Changes and DNA Fragmentation in IOA-Treated A549 Cells. Disorganization of the nucleus with chromatin changes induced by IOA in A549 cells was characterized using Hoechst 33342 staining. The A549 cells were exposed to 100 μM IOA for 24 h. Compared to vehicle (1% DMSO), most of which contained intact genomic DNA (Figure S1A), cells cultured with IOA had many cells with condensed chromatin (Figure S1B). Granulation of the nucleus appeared as fluorescent blue in the detail of the Hoechst 33342 stained cells (those from which vehicle was absent). Since nucleus granulation is a feature of the morphological change in apoptosis, these results suggest that IOA may induce apoptosis in A549 cells. Cells that exhibited reduced nuclear size, chromatin condensation, and nuclear fragmentation are considered apoptotic.[11] Next, we used an assay to study the effect of IOA on apoptosis by determining the amounts of nucleosomes in cytoplasm of cells. Figure 3B shows the time course of DNA fragmentation during continuous treatment with 1, 10, and 100 μM IOA for 6, 12, 18, and 24 h, respectively. DNA fragmentation of A549 was exhibited at 12 h and maximized at 24 h after the addition of IOA. In contrast to the control, when cells were treated with IOA, the levels of nucleosomes undergoing apoptosis increased from about 3.5-fold to 16-fold at 1 μM IOA and from 4.5-fold to 25-fold at 100 μM IOA from 6 to 24 h, respectively.

IOA Regulation of p53, p21/WAF1, $p27^{kip1}$, Bax, and Bcl-2 by ELISA Assay. We further examined the effect of IOA on cell-cycle regulation and apoptosis-related molecules by ELISA assay. As shown in Figure 4A, the up-regulation of p53 started to increase after 6 h of 100 μM IOA treatment, reaching a maximum expression at 12 h. A comparison of the apoptotic response results and induction of p53 results revealed that the up-regulation of p53 occurred at an early stage of the IOA-mediated antiproliferative process. Figure 4B shows the accumulation of p21/WAF1 in A549 cells by IOA. The induction of p21/WAF1 protein was apparent at 6 h and was enhanced over the next 18 h for 100 μM IOA. Moreover, the expression level of p21/WAF1 protein was greatly increased (at 18 h) after the maximal accumulation of p53 protein (at 12 h) in A549 cells. On the basis of these results, we hypothesize that the IOA-mediated cell-cycle arrest might occur through the induction of p21/WAF1 protein in a p53-dependent manner in A549 cells. In addition, we found $p27^{kip1}$ to be up-regulated in IOA-treated A549 cells, which started to increase after 6 h of treatment and reached its maximum expression at 18 h (Figure 4C). The effects of IOA were evaluated on the concentration of Bax and Bcl-2 in A549 cells compared to vehicle-treated control using different treatment times. As shown in Figure 5, IOA significantly increased Bax and decreased Bcl-2 levels in a time- and dose-dependent manner. The up-regulation of Bax and down-regulation of Bcl-2 by IOA exposure appeared after 6 h of IOA treatment. The increased Bax/Bcl-2 ratio induced by IOA treatment indicated apoptosis.

Effect of IOA on Change of Mitochondrial Membrane Potential ($\Delta\Psi_m$) and Release of Cytochrome *c*. As shown in Figure 6A, IOA induced mitochondrial transmembrane depolarization, represented as the decrease of mitochondrial membrane potential, which was represented by a decrease of fluorescent intensity of rhodamine 123 staining. In addition, IOA induced a significant increase in release of cytochrome *c* in human A459 cells in a time-dependent manner (Figure 6B). These data suggest that loss of mitochondrial membrane potential may be required for IOA-induced release of cytochrome *c* into the cytosol, which would later trigger the cleavage and activation of mitochondrial downstream caspases and the onset of apoptosis.

IOA Induces Apoptosis through Caspase-9 and Caspase-3 Activity and PARP Cleavage. Caspases, a group of cysteine proteases, have been demonstrated to play a pivotal role in the induction of apoptosis. To detect the caspase-9 and casapas-3 activity, we set out to explore whether IOA-induced apoptosis of

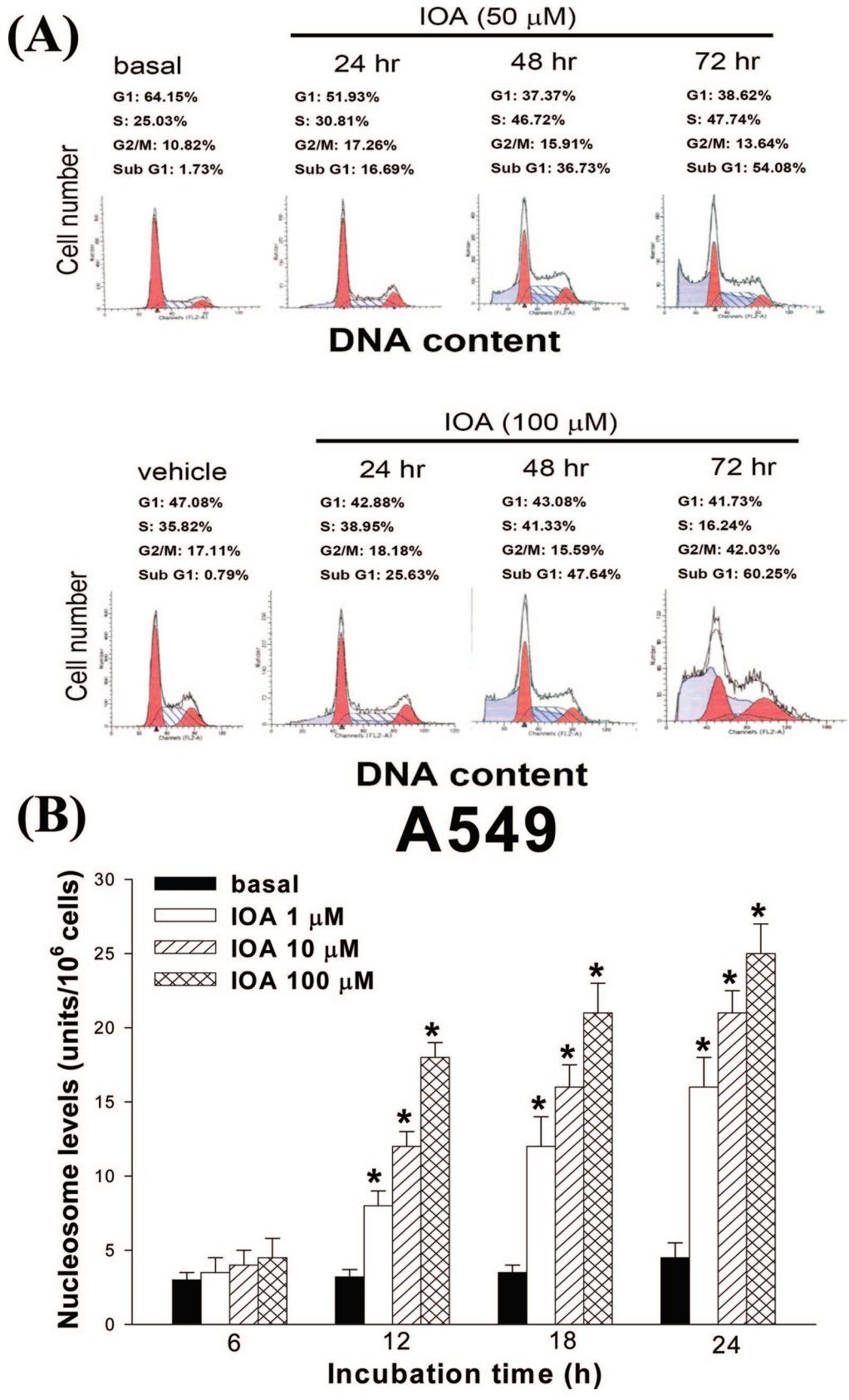

Figure 3. Effect of IOA on cell cycle of A549 cells. (A) A549 cells were treated with IOA (50 and 100 μM) for 24, 48, and 72 h, respectively. After treatment, cells were collected, fixed with methanol, stained with propidium iodide, and analyzed by flow cytometry. Data on each sample represent the percentage of cells in the G1, S, G2/M, and sub-G1 phases of the cell cycle, respectively. These experiments were performed at least three times. A representative experiment is presented. (B) A549 cells were cultured with 1, 10, and 100 μM IOA for 6, 12, 18, and 24 h, respectively. Cell lysates containing cytoplasmic oligonucleosomes of apoptotic cells were analyzed using a nucleosome ELISA kit. Each value represents the mean ± SE of three individual experiments. Statistically significant, $*p < 0.05$ to control group. ANOVA followed by Dunnett's test.

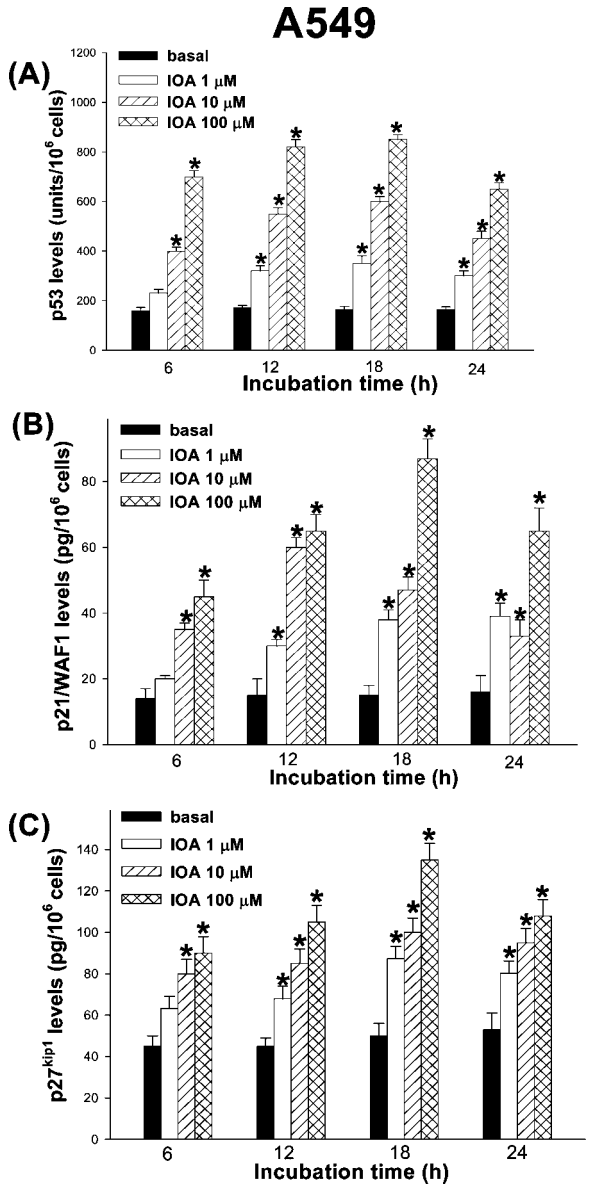

Figure 4. Effect of IOA on protein expression of p53, p21/WAF1, and $p27^{kip1}$. (A) Level of p53 in A549 cells; (B) level of p21/WAF1 in A549 cells; (C) level of $p27^{kip1}$ in A549 cells. A549 cells were treated with 1, 10, and 100 μM IOA. Lysates were prepared from these cells, and p53, p21/WAF1, and $p27^{kip1}$ levels were determined by p53 ELISA, p21WAF1 ELISA, and $p27^{kip1}$ ELISA kits, respectively. The detailed methods are described in the Experimental Section. Each value represents the mean ± SE of three individual experiments. Statistically significant, $*p < 0.05$ to control group. ANOVA followed by Dunnett's test.

A549 cells may be the result of a caspase-dependent mechanism. As shown in Figure 7, caspase-9 activity was clearly maximized at 6 h, earlier than caspase-3 and before the onset of apoptosis. Maximal activity was seen at 6 h, before the maximal levels of apoptosis were achieved (Figure 3B). When the cells were treated with 100 μM IOA, caspase-3 activity was slightly activated in a time-dependent manner (Figure 7B). In addition, 100 μM induced PARP (116 kDa; known as endogenous substrate for caspase-3 and a marker for apoptosis) cleavage to a 85 kDa C-terminal fragment in 24 h (data not shown), similar to caspase-3 activation.

Effect of IOA on Generation of ROS in Proliferation. In order to determine the chief component of ROS generation and the oxidative status of antioxidants and NO inhibitors on IOA treatment, we evaluated the effect of several ROS scavengers

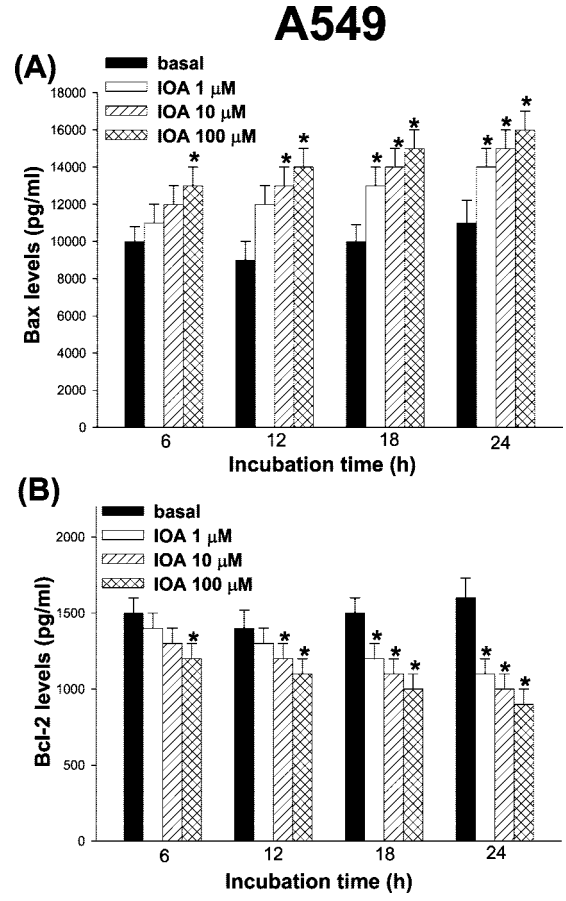

Figure 5. Effect of IOA on protein expression of Bax and Bcl-2. (A) Level of Bax; (B) level of Bcl-2. A549 cells were treated with 1, 10, and 100 μM IOA. Lysates were prepared from these cells, and Bax and Bcl-2 levels were determined by Bax and Bcl-2 ELISA kits, respectively. The steps are detailed in the Experimental Section. Each value represents the mean ± SE of three individual experiments. Statistically significant, $*p < 0.05$ to control group. ANOVA followed by Dunnett's test.

(catalase and mannitol), antioxidants (*N*-acetylcysteine (NAC) and Trolox), and NO inhibitors (dexamethasone and L-NAME) on IOA-induced intracellular DCF fluorescence in A549 cells. As shown in Figure S2A, A549 cells treated with 100 μM IOA had approximately 5.5-fold increases in DCF fluorescence intensity after 30 min treatment, compared to the untreated cells. However, catalase (a H_2O_2 scavenger), mannitol (a hydroxyl radical scavenger), dexamethasone, and L-NAME could significantly decrease intracellular DCF fluorescence in IOA-induced A549 cells. We also found that there was a DCF-fluorescence-diminishing effect for two antioxidants, NAC and Trolox. It is interesting to note that the lowest intracellular DCF fluorescence appeared with NAC treatment, suggesting that the chief ROS produced by IOA was H_2O_2. We further investigated the effects of the antioxidant NAC and the NO inhibitor L-NAME on IOA-induced antiproliferation in A549 cells (Figure S2B). We observed antiproliferation in IOA-treated, but not in NAC and L-NAME alone. On the other hand, IOA-induced antiproliferation was markedly more inhibited by pretreatment with the NAC than L-NAME.

IOA-Induced Inhibition of Migration and Invasion. To investigate whether IOA inhibits NSCLC metastasis, we conducted *in vitro* migration and invasion assays in A549 cells. We used IOA (1 and 10 μM), which had low cytotoxic activities within 1 day (Figure 2B), to evaluate the effects of IOA on the migration and invasion of A549 cells. The migration (Figure S3A) and invasion (Figure S3B) of A549 cells were significantly inhibited by pretreatment with IOA. The reduction in migration was concentration-

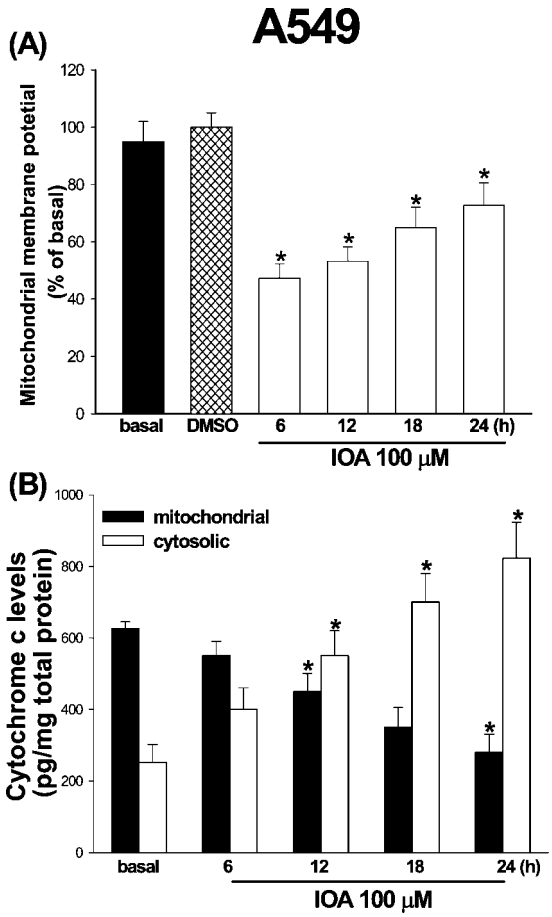

Figure 6. Effect of IOA on $\Delta\Psi_m$ reduction and cytochrome *c* release of A549 cells. (A) Cells exposed to 100 μM IOA or not for 24 h were incubated with rhodamine 123. Then, the fluorescence intensity was measured. (B) Level of cytochrome *c* protein in A549 cells. A549 cells were treated with 100 μM IOA. Lysates were prepared from these cells and cytochrome *c* levels were determined by cytochrome *c* ELISA kit. Each value represents the mean ± SE of three individual experiments. Statistically significant, $*p < 0.05$ to control group. ANOVA followed by Dunnett's test.

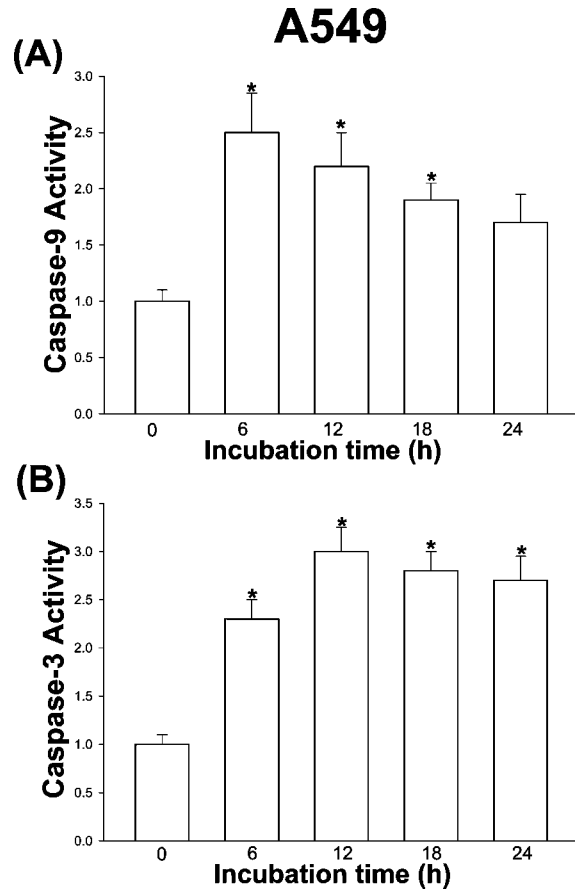

Figure 7. Effect of 100 μM IOA on time-dependent activation of caspase-9 and caspase-3 of A549 cells. Enzymatic activity assay of caspase-9 (A) and caspase-3 (B) was determined by incubation with the colorimetric peptide substrate Ac-DEVD-pNA and the fluorogenic peptide substrate Ac-DEVD-AFC, respectively, as described in the Experimental Section. Each value represents the mean ± SE of three individual experiments using the 0 h group as controls. Statistically significant, $*p < 0.05$ to 0 h group. ANOVA followed by Dunnett's test.

dependent. In contrast, pretreatment with vehicle had no significant effects on the migration and invasion of the cells. Moreover, a slight reduction in cell invasion was also found to be concentration-dependent. IOA (1 μM)-induced inhibition had more potential on migration than on invasion. However, 10 μM IOA-induced anti-migration and anti-invasion were significantly abolished by pre-treatment with antioxidant NAC.

Many natural compounds, especially plant products and dietary constituents, have been found to possess chemopreventive activities both *in vitro* and *in vivo*.[12] Previous studies have demonstrated that IOA is a potent cytotoxic compound capable of inducing apoptosis and cell arrest in human hepatoma cancer cells Hep G2 and two breast cancer cell lines, MCF-7 and MDA-MB-231.[2,3] To date, the molecular events necessary for IOA-induced cell death in lung cancer have not been clearly identified.

In the present study, we investigated the possible mechanisms via IOA, a novel constituent isolated from the levels of C. *kotoense*, underlying the induction of apoptosis, antiproliferation, enhancement of reactive oxygen species, and inhibition of both migration and invasion in NSCLC A549 cells, resistant to radiation and chemotherapy. Signals leading to activation of a variety of gene products, such as P53, P21, P27, and Bcl-2 family proteins consisting of Bax, have been found to be important in the regulation and execution of apoptosis induced by various stimuli.[13] We found an association between IOA-induced apoptosis and increased expression of P53, suggesting P53 plays a pivotal role in this process (Figure 4).

P53 is known to cause cell-cycle arrest or induce apoptosis.[14–17] Gene-targeting strategies have established that one critical mediator of the p53-mediated G1 arrest response is p21/WAF1.[15,16] Up-regulation of P21/WAF1/CIP1 by different chemopreventive agents is associated with G2/M phase arrest in the cell cycle.[18] Because IOA-induced apoptosis in A549 cells is associated with increased expressions of P53 and P21/WAF1/CIP1, the mechanism of cell-cycle arrest on the cell death signaling by IOA cannot be ruled out. In addition, some reports have shown that overexpression of $p27^{Kip1}$ induces apoptosis in various cell lines and in lung cancer cells.[19] $p27^{Kip1}$ negatively regulates transition from the G1 to the S phase of the cell cycle by binding to G1 cyclin−CDK complexes,[20] resulting in inhibition of proliferation. The reduced levels of $p27^{Kip1}$ have been reported to be an independent prognostic factor correlating with the overall survival periods in carcinomas such as NSCLC. Once a cytotoxic agent causes DNA damage, p53 accumulates in the nucleus and it functions as a transcription factor to modulate its target genes such as p21/WAF1 and Bax.[21] Bax counteracts the antiapoptotic effects of Bcl-2 by forming Bax/Bcl-2 heterodimers. The translocation of Bax to mitochondria can alter the outer membrane permeability, which subsequently activates the caspase cascade, leading to apoptotic death. Our data revealed that IOA induced p53 expression in a time-dependent manner, which

was coincidentally correlated with the up-regulation of downstream affectors, such as p21/WAF1 and Bax (Figure 4). The up-regulated p21/WAF1 and Bax subsequently caused G2/M phase arrest in cell-cycle progression and resulted in mitochondria-dependent apoptotic cell death. Our results further demonstrated that the G2/M phase cell-cycle arrest and apoptosis induced by IOA involve multiple pathways related to p53, p21, and $p27^{Kip1}$. Because p53 is critical in the maintenance of genome integrity in that it regulates the cell cycle (p21/WAF1 and cyclin G), DNA damage, and apoptosis (Bax), restoring apoptosis via regulation of p53 is an important strategy in cancer gene therapy.[22] Our data show that IOA induces p53 in A549 cells, suggesting that p53 is critical to the induction of cell-cycle arrest and apoptosis mediated by IOA.

The induction of G2/M phase cell-cycle arrest and apoptosis by IOA may be explained by its antiproliferation resulting from an apoptotic mechanism. Both $p27^{Kip1}$ and p21 are important cell-cycle regulating factors, and they play an important role in cancer cell apoptosis and cell-cycle arrest.[20] The results of the caspase activity assays showed that IOA induced activation of caspase-9 and caspase-3 in a dose-dependent manner, suggesting that IOA may have also induced apoptosis via the traditional nuclear DNA damage pathways. However, the IOA-induced activity of caspase-9 and caspase-3 and release of cytochrome *c* indicate that an earlier mitochondria-related apoptosis was activated by IOA.

Since the Bcl-2 family of proteins is regarded as a key regulator of apoptosis and is known to play a critical role in the control of mitochondrial integrity, we investigated the influence of IOA on Bcl-2, Bax, $\Delta\Psi_m$, and cytochrome *c* expression levels in A549 cells. Bcl-2 is seen as antiapoptotic, whereas Bax can be regarded as pro-apoptotic; therefore, an increased ratio of pro-apoptotic Bax to antiapoptotic Bcl-2 can be associated with apoptosis. Bax and Bcl-2 are responsible for either the induction or prevention of mitochondrial membrane permeability, which is important in regulating the release of cytochrome *c* from motochondria into the cytosol, leading to activation of caspase cascade such caspase-9 and caspase-3 and induction of apoptotic cell death.[23] In this study, the IOA-induced apoptosis in A549 cells was accompanied by up-regulation of Bax and the down-regulation of Bcl-2. The maximal Bax/Bcl-2 ratio induced by 100 μM IOA was 1.78-fold, normalized against the Bcl-2 level at 24 h. Furthermore, IOA-induced A549 cells released cytochrome *c* to the cytosol, which subsequently mediated caspase-9 and caspase-3 activation and cell apoptosis. The cleavage of PARP, a 116 kDa nuclear enzyme downstream of caspase-3, produces an 85 kDa fragment, providing further evidence that IOA treatment of A549 cells induced the activitation of caspase-9 and caspase-3 (Figure 7). The generation of ROS may contribute to mitochondrial damage and lead to cell death by acting as an apoptotic signaling molecule.[24] Several previous studies indicate that IOA acts as a ROS generator to increase the susceptibility of tumor cells to apoptosis.[2,3] We found that, in addition to its effect on $\Delta\Psi_m$, IOA caused an increase in ROS production in A549 cells. The IOA-induced increase in ROS and antiproliferation in A549 cells are apparently dependent on ROS generation because the IOA-induced increase in ROS can be abolished or attenuated by several ROS scavengers, such as catalase and mannitol, antioxidants, such as NAC and Trolox, and NO inhibitors, such as dexamethasone and L-NAME. In addition, we found that IOA-induced antiproliferation in A549 cells was also abolished by the antioxidant NAC. In addition, IOA (Figure 1) is an α-methylene lactone moiety (though not a sesquiterpene) and can, therefore, act as a Michael-reaction acceptor in cells. The reversal of effects by NAC that we observed could be a result of competition with cellular targets of such a mechanism. Further studies are needed to clarify this.

Metastasis is the major cause of mortality. Because ROS have been recently proposed to be involved in tumor metastasis,[25] our studies support the specific, essential role of IOA-induced ROS in cell migration and invasion. We found the IOA-induced increase in ROS production and the A549 cell migration and invasion phenomenon could be abolished or attenuated by IOA treatment. Furthermore, the antioxidant NAC may prevent IOA-induced cell migration and invasion (Figure S3), suggesting that IOA-induced antimigration and anti-invasion are involved in the production of ROS.

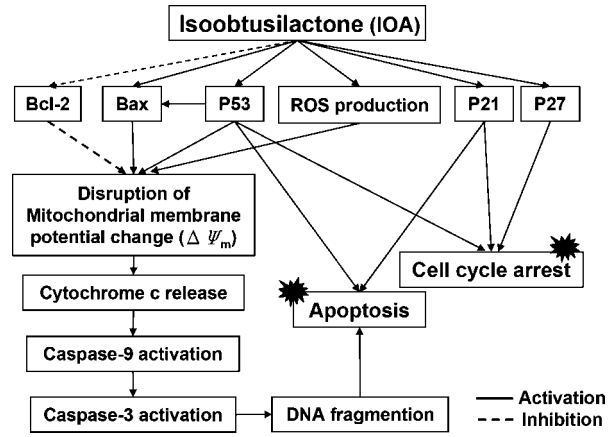

Figure 8. Schematic drawing representing possible mechanisms underlying IOA-induced apoptosis and cell arrest in human NSCLC A549 cells. IOA-induced apoptosis is mediated through the up-regulation of P53, P21, P27, and Bax and/or the down-regulation of Bcl-2, and/or mediates ROS generation, resulting in the reduction of mitochondrial membrane potential, release of cytochrome *c* into the cytosol, activation caspase-9 and caspase-3, and ultimately apoptosis.

As can be seen in Figure 8, the present study has allowed us to make several important conclusions. (1) We have demonstrated the therapeutic potential of IOA for NSCLC A549 cells because IOA has antiproliferative and apoptosis properties in A549 cells. (2) IOA can inhibit cell-cycle arrest progression at G2/M and apoptosis by increasing p53, p21, and p27 expression and increasing Bax/Bcl-2 ratio. (3) IOA can disrupt the function of mitochondria at the early stage of apoptosis and subsequently activate caspase-9 and caspase-3 activation through the release of cytochrome *c*. (4) IOA-induced cell antiproliferation, antimigration, and anti-invasion effects in A549 cells are mediated by the production of ROS. Together these findings characterize a basic mechanism through which IOA has chemotherapeutic properties relevant to the treatment of lung cancer. Further investigation along these lines of inquiry should be given high priorty, as IOA has potentially important therapeutic applications.

Experimental Section

General Experimental Procedures. Optical rotations were measured using a JASCO DIP-370 digital polarimeter. UV spectra were obtained in MeCN using a JASCO V-530 spectrophotometer. The IR spectra were measured on a Hitachi 260-30 spectrophotometer. ^{1}H NMR spectra were referenced to residual $CDCl_3$ at δ 7.27, and ^{13}C NMR were referenced to the center line of $CDCl_3$ at δ 77.0. DEPT NMR spectra were obtained using a Unity Plus Varian NMR spectrometer. LR-FABMS and LREIMS were obtained with a JEOL JMS-SX/SX 102A mass spectrometer or a Quattro GC-MS spectrometer with a direct inlet system. Silica gel 60 (Merck, 230−400 mesh) was used for column chromatography. Precoated silica gel plates (Merck, Kieselgel 60 F-254, 0.20 mm) were used for analytical TLC, and precoated silica gel plates (Merck, Kieselgel 60 F-254, 0.50 mm) were used for preparative TLC. Spots were detected by spraying with 50% H_2SO_4 and then heating on a hot plate.

Plant Material. The leaves of *C. kotoense* were obtained from Fooyin University of Kaohsiung in Taiwan. The voucher specimen was characterized by Dr. Pei-Fang Lee of the Graduate Institute of Biotechnology, Fooyin University, Kaohsiung County, Taiwan, and deposited in the Basic Medical Science Education Center, Fooyin University, Kaohsiung County, Taiwan.

Extraction and Isolation. The air-dried leaves of *C. kotoense* (11.0 kg) were extracted with methanol (80 L × 6) at room temperature, and the methanol extract (201.2 g) was obtained through concentration under reduced pressure. The methanol extract, suspended in H_2O (1 L), was partitioned with $CHCl_3$ (2 L × 5) to give fractions soluble in $CHCl_3$ (112.4 g) and H_2O (56.8 g). The $CHCl_3$-soluble fraction (112.4 g) was eluted into five fractions with *n*-hexane−EtOAc−acetone by silica gel chromatography. Fraction 1 (5.31 g) was subjected to silica gel chromatography by eluting with *n*-hexane−EtOAc (20:1), then enriched with EtOAc to furnish 10 fractions. Fraction 4 (3.12 g) was eluted with *n*-hexane−EtOAc (40:1) using silica gel chromatography and enriched gradually with EtOAc to obtain three fractions. Fraction 2 (3.01 g) was further purified by silica gel CC and preparative TLC (*n*-hexane−EtOAc (30:1)) using *n*-hexane−EtOAc (40:1) to yield pure isoobtusilactone A (2.88 g), which was identified by spectroscopic data analysis and compared with literature values.[26]

Cell Culture. The human NSCLC cell line A549 (American Type Culture Collection, ATCC) was grown routinely at 37 °C and 5% CO_2 in RPMI-1640 medium supplemented with 10% FBS, 100 U/mL penicillin, 100 μg/mL streptomycin, and 0.25 μg/mL amphotericin B.

Drugs and Chemicals. 3-[4,5-Dimethylthiazol-2-yl]-2,5-diphenyl tetrazolium bromide (MTT), dimethyl sulfoxide (DMSO), ribonuclease (RNase), propidium iodide (PI), *N*-acetyl-L-cysteine (NAC), mannitol, dexamethasone, and N^{ω}-nitro-L-arginine methyl ester (L-NAME) were obtained from Sigma-Aldrich Chemical Co. (St. Louis, MO). RPMI-1640, fetal bovine serum (FBS), penicillin G, streptomycin, amphotericin B, trypan blue (TB), and all other cell culture reagents were obtained from Gibco BRL Life Technologies (Grand Island, NY). 2′,7′-Dichlorodihydrofluorescein diacetate (DCFH-DA) was purchased from Molecular Probes (Eugene, OR). Nucleosome ELISA kits, caspase-9 substrate (Ac-LEHD-pNA), and caspase-3 substrate (Ac-DEVD-AFC) were purchased from Calbiochem (San Diego, CA) and BD Biosciences (San Jose, CA). p21/WAF1, $p27^{kip1}$, p53, cytochrome *c*, Bax, and Bcl-2 ELISA kits were purchased from Assay Designs (Ann Arbor, MI). All drugs and reagents were dissolved in distilled H_2O unless otherwise noted. IOA was dissolved in DMSO at 1 M stock and serially diluted with distilled H_2O and vehicle (contains 1% DMSO in sterilized distilled H_2O).

Trypan Blue Dye Exclusion Assay. A549 cells (1×10^5) were seeded onto a 60 mm culture dish. The next day cells were treated with 100 μM IOA for 12, 24, 48, and 72 h, respectively. The treated cells were then harvested, washed twice with phosphate-buffered saline (PBS), concentrated to 150 μL, transferred to 20 μL of cell suspension, and stained with 20 μL of TB. This method is based on the principle that live (viable) cells do not take up certain dyes, whereas dead (nonviable) cells do. The percentage of unstained viable cells was counted using the microscope.

Cell Proliferation Assay. MTT assay was used to measure the proliferation response. MTT cleavage into a blue-colored formazan product by the mitochondrial enzyme succinyl dehydrogenase occurs exclusively in living cells. Cells were grown in growth medium plus 10% FBS in 48-well plates (until 70−80% confluence) and then treated with various concentrations of IOA and incubated for 24, 48, and 72 h, respectively. An the end of the incubation period, an MTT assay was performed. Briefly, 20 μL of a 5 mg/mL MTT solution were added to each well, and the cells were maintained at 37 °C for 3 h. After removing the medium, 200 μL of 2-propanol was added to solublize the resulting intracellular purple formazan product. The plates were shaken for 5 min. The optical density at 570 nm was measured with a screening multiwell spectrophotometer enzyme-linked immunosorbent assay (ELISA) reader and compared with that of control wells. The reference wavelength was 650 nm.

Cell-Cycle Analysis. A549 cells (5×10^5) were seeded onto a 60 mm culture dish. The next day, cells were treated with 50 and 100 μM IOA for 24, 48, and 72 h, respectively. After IOA treatment, adherent and floating A549 cells were pooled, washed with PBS, fixed in PBS−MeOH (1:2, v/v) solution, and maintained at 4 °C for at least 18 h. After an additional wash with PBS, the cell pellets were stained with the fluorescent probe solution containing PBS, 50 μg of PI/mL, and 50 μg of DNase-free RNaseA/mL for 30 min at room temperature in the dark. Cells were then analyzed using a FACS-Calibur cytometer (Becton Dickinson, San Jose, CA) with excitation set at 488 nm. Gating out of doublets and clumps was done by pulse processing and collecting fluorescence emission above 580 nm. The percentage of DNA damaged cells was defined as the percentage of cells in the subdiploid region (sub-G1) of the DNA distribution histograms.

Morphological Changes (Chromatin Condensation). To access the DNA, chromatin morphologic features were detected by Hoechst 33342 staining. Briefly, cells were treated with IOA for 24 h, fixed with 3.7% paraformaldehyde (pH 7.4), washed twice in PBS, and incubated with Hoechst 33342 (5 μg/mL) at 37 °C for 1 h. After washing with PBS, the stained nuclei were observed and photographed using an Olympus fluorescence microscope (Olympus IX 70, Japan) at 480 nm. Cells exhibiting reduced nuclear size, chromatin condensation, and nuclear fragmentation were considered apoptotic.

Measurement of Apoptosis by ELISA. The induction of apoptosis by IOA was assayed using a nucleosome ELISA kit. This kit uses a photometric enzyme immunoassay quantitatively determining the formation of cytoplasmic histone-associated DNA fragments (mono- and oligonucleosomes) after apoptotic cell death. A549 cells were treated with 1, 10, and 100 μM IOA for 6, 12, 18, and 24 h, respectively. The samples of cell lysate were placed in a 96-well plate (1×10^6/well). The induction of apoptosis was evaluated by assessing the enrichment of nucleosome in cytoplasm and determined following manufacturer's directions.

Measurement the Levels of p53, p21/WAF1, $p27^{kip1}$, Bcl-2, and Bax. p53, p21/WAF1, $p27^{kip1}$, Bcl-2, and Bax ELISA kits were used to detect p53, p21, p27, Bcl-2, and Bax levels. Briefly, A549 cells were treated with 1, 10, and 100 μM IOA for 6, 12, 18, and 24 h, respectively. The samples of cell lysate were placed in 96-well (1×10^6/well) microtiter plates coated with monoclonal detective antibodies and incubated for 1 h (p21/WAF1, Bcl-2, and Bax) or 2 h (p53 and $p27^{kip1}$) at room temperature. After removing unbound material by washing with washing buffer (50 mM Tris, 200 mM NaCl, and 0.2% Tween 20), horseradish peroxidase conjugated streptavidin was added to bind to the antibodies. Horseradish peroxidase catalyzed the conversion of a chromogenic substrate (tetramethylbenzidine) to a colored solution with color intensity proportional to the amount of protein present in the sample. The absorbance of each well was measured at 450 nm, and concentrations of p53, p21/WAF1, $p27^{kip1}$, Bcl-2, and Bax were determined by interpolation from standard curves obtained with known concentrations of standard proteins.

Measurement of Mitochondrial Membrane Potential ($\Delta\Psi_m$). Mitochondrial membrane potential ($\Delta\Psi_m$) was measured by the incorporation of cationic fluorescent dye, rhodamine 123. After 6, 12, 18, and 24 h incubation in normal medium with or without treatment with 100 μM IOA, the normal medium was changed to a serum-free medium containing 10 μM rhodamine 123 and incubated for 15 min at 37 °C. The cells were then collected and the flurescence intensity was analyzed within 15 min by a spectrophotofluorimeter (FLUOstar OPTIMA, Germany, 490 nm excitation and 515 nm emission).

Measurement of Cytochrome *c* Levels on Cytosolic and Mitochondrial Fractions. Cytochrome *c* ELISA kits were used to detect cytochrome *c*. Briefly, A549 cells were treated with 100 μM IOA or with DMSO (for a vehicle control) for 6, 12, 18, and 24 h, respectively, at 37 °C. Cells were harvested and centrifuged briefly at 800*g*. The supernatant was discarded. The cell pellet was resuspended, washed with PBS, and centrifuged at 1000*g* for 5 min, after which the supernatant was discarded. The cell pellet was resuspended with digitonin cell permeabilization buffer (250 mM sucrose, 137 mM NaCl, 70 mM KCl, 4.3 mM Na_2HPO4, 1.4 mM K_2HPO4, 0.2 mg/mL digitonin, and 0.1% Hydorol M), vortexed, and incubated on ice for 5 min. Cells were then centrifuged at 1000*g* for 5 min at 4 °C. The supernatants were saved, as these contained the cytosolic fraction of cytochrome *c*. The remaining pellet was then resuspended with cell lysis buffer (50 mM Tris HCl, pH 7.4, 150 mM NaCl, 1 mM EDTA, 1 mM EGTA, 1% Triton X-100, 1% sodium deoxycholate, and 0.1% SDS), vortexed, and incubated on ice for 5 min. The lysate was vortexed and centrifuged at 10000*g* for 10 min at 4 °C as mitochondrial fractions. Like the above ELISA assay methods, two fractions were run using a modification of the manufacturer's directions for performing the assay.

Measurement of Casapase-9 and Caspase-3 Activity. To measure the enzymatic activity of caspase-9 and caspase-3, A549 cells were treated with 100 μM IOA for 6, 12, 18, and 24 h, respectively, and then were washed with PBS and collected by centrifugation. The cell pellets were lysed in lysis buffer (1% Triton X-100, 0.32 M sucrose, 5 mM EDTA, 1 mM phenylmethylsulfonyl fluoride (PMSF), 1 μg/μL aprotinin, 1 mM leupetin, 2 mM dithiothreitol, and 10 mM Tris-HCl)

on ice for 1 h and were then centrifuged for 30 min at 13200*g*. The assay was based on the ability of the active enzyme to cleave the chromophore and fluorophore from the enzyme substrates, Ac-DEVD-pNA and Ac-DEVD-AFC, respectively. The cell lysates (80 μg) were incubated with peptide substrate in assay buffer (100 mM NaCl, 20 mM PIPES, 10 mM dithiothreitol (DTT), 1 mM EDTA, 0.1% CHAPS, 10% sucrose, pH 7.2) at 37 °C for 1 h in the dark. The Ac-DEVD-pNA cleavage (paranitroaniline) was measured in a multiwell spectrophotometer ELISA reader at a wavelength of 405 nm. Otherwise, the Ac-DEVD-AFC cleavage fluorogenic AFC was measured in a spectrophotofluorimeter (FLUOstar OPTIMA, 400 nm excitation and 520 nm emission). Results are represented as the percentage change of the activity compared to the untreated control.

Determination of Intracellular H_2O_2 and/or Peroxide (ROS). Production of intracellular H_2O_2 and/or peroxide was detected by flow cytometry using cell-permeable probe DCFH-DA. This dye is a stable compound that readily diffuses into cells and yields dichlorodihydrofluorescein (DCFH) in the presence of H_2O_2 and/or peroxide. A549 cells (1×10^6) were cultured in 60 mm culture dishes. The culture medium was replaced with new medium when the cells were 80% confluent. They were then exposed to 100 μM IOA for 30 min. After being treated with IOA, cells were treated with 10 μM DCFH-DA for another 30 min in the dark, washed once with PBS, detached by trypsinization, collected by centrifugation, and suspended in PBS. The intracellular H_2O_2 and/or peroxide (ROS), as indicated by the fluorescence of dichlorofluorescein (DCF), was measured using a Becton-Dickinson FACS-Calibur flow cytometer with excitation and emission settings of 488 and 525−550 nm, respectively. For antioxidants and NO inhibitor studies, A549 cells were first pretreated with either NAC (10 mM), catalase (200 U/mL), mannitol (50 mM), dexamethasone (10 μM), Trolox (50 μM), or L-NAME (100 μM) for 30 min, followed by incubation with 100 μM for another 30 min, and then analyzed as described above. To explore the possibility that IOA induced intracellular ROS in antiproliferation, the A549 cells were pretreated with NAC (10 mM) and L-NAME (100 μM) 2 h before treatment with IOA, followed by 100 μM IOA treatment for 24 h. A549 cells proliferation response was determined by MTT assay as described above.

Migration and Invasion Assays. The ability of A549 cells to migrate was examined in cell culture chamber inserts (8.0 μM pore size; Chemicon QCM 24-well cell migration assay kit, Upstate & Chemicon, CA). Following manufacture's directions for performing the migration assay, 5×10^4 cells in serum-free medium were added to the upper chamber, while the lower compartments were filled with 10% FBS medium, incubated for 24 h at 37 °C in a CO_2 incubator (5% CO_2). The cells/media were carefully removed from the top side of the insert. The migration insert was placed into a cell stain solution and incubated for 20 min at room temperature. The insert was dipped into water several times, and a cotton-tipped swab was used to remove the nonmigratory cell layer from the interior insert. The insert was allowed to air dry and then transferred to extraction buffer for 15 min at room temperature. The 100 μL extracted stain dye was transferred to a 96-well plate for colorimetric analysis using optical density set at 560 nm. Otherwise, the invasion assay was done in the same way except for coating the Transwell units with Matrigel (BioCoat Matrigel invasion chamber, Becton Dickinson Labware, Bedford, MA). The invasion methods were assayed according to manufacture's directions but modified as described above for the migration assay. The results are expressed as the percentage of cells that migrated or invaded compared with that of control cells.

Statistical Evaluation of Data. The results are expressed as mean ± SE. Statistical differences were estimated by one-way analysis of variance (ANOVA) followed by Dunnett's test. A p value of 0.05 was considered significant. Analysis of the data and plotting of the figures were performed with the aid of software (SigmaPlot Version 8.0 and SigmaStat Version 2.03, Chicago, IL) run on an IBM-compatible computer.

Acknowledgment. This study was supported by grants NSC-95-2320-B-037-052-MY2 and NSC-94-2320-B-242-013 to R.-J.L. from the National Science Council, Taiwan.

Supporting Information Available: The effects of IOA-induced A549 cells' morphological changes (chromatin condensation) (Figure S1), IOA-induced ROS increase (Figure S2), and IOA-induced inhibition of migration and invasion (Figure S3) data are available free of charge via the Internet at http://pubs.acs.org

References and Notes

(1) Chen, F. C.; Peng, C. F.; Tsai, I. L.; Chen, I. S. *J. Nat. Prod.* **2005**, *68*, 1318–1323.
(2) Kuo, P. L.; Chen, C. Y.; Hsu, Y. L. *Cancer Res.* **2007**, *67*, 7406–7420.
(3) Chen, C. Y.; Liu, T. Z.; Chen, C. H.; Wu, C. C.; Cheng, J. T.; Yiin, S. J.; Shih, M. K.; Wu, M. J.; Chern, C. L. *Food Chem. Toxicol.* **2007**, *45*, 1268–1276.
(4) Kuo, Y. C.; Lu, C. K.; Huang, L. W.; Kuo, Y. H.; Chang, C.; Hsu, F. L.; Lee, T. H. *Planta Med.* **2005**, *71*, 412–415.
(5) Tsai, I. L.; Hung, C. H.; Duh, C. Y.; Chen, I. S. *Planta Med.* **2002**, *68*, 142–145.
(6) Garcez, F. R.; Garcez, W. S.; Martins, M.; Matos, M. F.; Guterres, Z. R.; Mantovani, M. S.; Misu, C. K.; Nakashita, S. T. *Planta Med.* **2005**, *71*, 923–927.
(7) Cordes, N.; Beinke, C.; Plasswilm, L.; van Beuningen, D. *Strahlenther Onkol.* **2004**, *180*, 157–164.
(8) Kim, P. K.; Park, S. Y.; Koty, P. P.; Hua, Y.; Luketich, J. D.; Billiar, T. R. *J Thorac. Cardiovasc. Surg.* **2003**, *125*, 1336–1342.
(9) Peters, G. J.; Smorenburg, C. H.; Van Groeningen, C. J. *16 Suppl.* **2004**, *4*, 25–30.
(10) Kurbacher, C. M.; Mallmann, P. K. *Anticancer Res.* **1998**, *18*, 2203–2210.
(11) Martin, S. J.; Green, D. R.; Cotter, T. G. *Trends Biochem. Sci.* **1994**, *19*, 26–30.
(12) Kelloff, G. J.; Crowell, J. A.; Steele, V. E.; Lubet, R. A.; Malone, W. A.; Boone, C. W.; Kopelovich, L.; Hawk, E. T.; Lieberman, R.; Lawrence, J. A.; Ali, I.; Viner, J. L.; Sigman, C. C. *J. Nutr.* **2000**, *130*, 467S–471S
(13) Taguchi, T.; Kato, Y.; Baba, Y.; Nishimura, G.; Tanigaki, Y.; Horiuchi, C.; Mochimatsu, I.; Tsukuda, M. *Oncol. Rep.* **2004**, *11*, 421–426.
(14) Hsu, Y. L.; Cho, C. Y.; Kuo, P. L.; Huang, Y. T.; Lin, C. C. *J. Pharmacol. Exp. Ther.* **2006**, *318*, 484–494.
(15) May, P.; May, E. *Oncogene* **1999**, *18*, 7621–7636.
(16) Bennett, W. P.; Hussain, S. P.; Vahakangas, K. H.; Khan, M. A.; Shields, P. G.; Harris, C. C. *J. Pathol.* **1999**, *187*, 8–18.
(17) Donehower, L. A.; Harvey, M.; Slagle, B. L.; McArthur, M. J.; Montgomery, C. A., Jr.; Butel, J. S.; Bradley, A. *Nature* **1992**, *356*, 215–221.
(18) Harvat, B. L.; Wang, A.; Seth, P.; Jetten, A. M. *J. Cell. Sci.* **1998**, *111*, 1185–1196.
(19) Wang, X.; Gorospe, M.; Huang, Y.; Holbrook, N. J. *Oncogene* **1997**, *15*, 2991–2997.
(20) Sherr, C. J.; Roberts, J. M. *Genes Dev.* **1995**, *9*, 1149–1163.
(21) Kim, Y. A.; Lee, W. H.; Choi, T. H.; Rhee, S. H.; Park, K. Y.; Choi, Y. H. *Int. J. Oncol.* **2003**, *23*, 1143–1149.
(22) Sasaki, Y.; Morimoto, I.; Ishida, S.; Yamashita, T.; Imai, K.; Tokino, T. *Gene Ther.* **2001**, *8*, 1401–1408.
(23) Slee, E. A.; Harte, M. T.; Kluck, R. M.; Wolf, B. B.; Casiano, C. A.; Newmeyer, D. D.; Wang, H. G.; Reed, J. C.; Nicholson, D. W.; Alnemri, E. S.; Green, D. R.; Martin, S. J. *J. Cell Biol.* **1999**, *144*, 281–292.
(24) Simbula, G.; Columbano, A.; Ledda-Columbano, G. M.; Sanna, L.; Deidda, M.; Diana, A.; Pibiri, M. *Apoptosis* **2007**, *12*, 113–123.
(25) Wu, W. S. *Cancer Metastasis Rev.* **2006**, *25*, 695–705.
(26) Anderson, J. E.; Ma, W. W.; Smith, D. L.; Chang, C. J.; McLaughlin, J. L. *J. Nat. Prod.* **1992**, *55*, 71–83.

NP070620E